J. Braz. Chem. Soc., Vol. 20, No. 5, 954-966, 2009.
Printed in Brazil - ©2009 Sociedade Brasileira de Química
0103 - 5053 $6.00+0.00

Article

Synthesis, Characterization and use of Nb_2O_5 based Catalysts in Producing Biofuels by Transesterification, Esterification and Pyrolysis

Rodrigo F. Brandão, Rafael L. Quirino, Vinicius M. Mello, André P. Tavares, Antônio C. Peres, Flávia Guinhos, Joel C. Rubim and Paulo A. Z. Suarez*

Instituto de Química, Universidade de Brasília, Campus Universitário Darcy Ribeiro, CP 4478, 70904-970 Brasília-DF, Brazil

Nb_2O_5/HX (X = HSO_4^-, $H_2PO_4^-$, NO_3^-) foram obtidos após o tratamento do $Nb_2O_5{\cdot}xH_2O$ com ácido sulfúrico, fosfórico, nítrico, sendo investigados juntamente com Nb_2O_5 e $Nb_2O_5{\cdot}xH_2O$ como catalisadores na reação de transesterificação, esterificação e pirólise de óleos vegetais. Os catalisadores foram caracterizados por análise térmica (DTA-TGA), espectroscopia (DRX, FT-IV e FT-Raman), área superficial (BET), e determinada acidez (Ho) pela titulação com *n*-butilamina utilizando o método Hammet. Após o tratamento ácido, todas as áreas superficiais e a acidez decresceram comparadas com o $Nb_2O_5{\cdot}xH_2O$ utilizado inicialmente no tratamento. A única exceção foi a alta acidez verificada quando o ácido nítrico foi utilizado. Entre os catalisadores testados, o Nb_2O_5/H_3PO_4 apresentou boa atividade na reação de alcoólise do óleo de soja com diferentes alcoóis (metanol, etanol, 2-propanol, *n*-butanol). Todos os sólidos testados demonstraram estabilizar ácidos carboxílicos durante a pirólise. Finalmente, o uso de Nb_2O_5/H_3PO_4 e Nb_2O_5/H_2SO_4 como catalisador na reação de esterificação demonstrou melhor atividade que o Nb_2O_5 e $Nb_2O_5{\cdot}xH_2O$.

Nb_2O_5/HX (X = HSO_4^-, $H_2PO_4^-$, NO_3^-) compounds were obtained from the treatment of niobium acid ($Nb_2O_5{\cdot}xH_2O$) with sulfuric, phosphoric, and nitric acids as well as Nb_2O_5 and $Nb_2O_5{\cdot}xH_2O$ have been investigated as catalysts for the transesterification, esterification and pyrolysis of vegetable oils. The compounds were characterized by thermal analysis (DTA-TGA), spectroscopy (DRX, FT-IR and FT-Raman), surface area (BET) and the acidity (Ho) determined by *n*-butylamine titration using the Hammet´s indicator method. It was observed that after the acid treatment both the surface area and the acidity decreased as compared to the starting $Nb_2O_5{\cdot}xH_2O$. The only exception was a higher acidity verified when nitric acid was used. Among the catalyst investigated, the Nb_2O_5/H_3PO_4 presented the highest activity in the alcoholysis of soybean oil with different mono-alcohols (methanol, ethanol, 2-propanol, *n*-butanol). All tested solids seemed to stabilize the carboxylic acids formed during the pyrolysis, yielding higher acid numbers for the obtained products. Finally, the use of Nb_2O_5/H_3PO_4 and Nb_2O_5/H_2SO_4 as catalysts for the esterification showed better activity than $Nb_2O_5{\cdot}xH_2O$ and Nb_2O_5.

Keywords: esterification, transesterification, pyrolysis, niobium compounds

Introduction

Due to economical and ecological reasons, the study of alternative sources of energy has been intensified in the last years.[1-5] In this context, the use of derivatives from triglycerides and fatty acids such as methyl- or ethyl fatty acid esters and hydrocarbons has received special attention as alternative fuels for diesel engines.[6-8] The main studied processes to obtain biofuels from triglycerides and fatty acids are depicted in Figure 1.

*e-mail: psuarez@unb.br

As in many other countries, the external dependence on imported diesel fuel and the present petroleum crisis have increased the discussion in Brazil in the sense of start using alternatives to diesel fuel.[9] In this sense, the use of fatty acid derived compounds is the main alternative for a large petroleum diesel substitution program.

The pyrolysis of vegetable oils has been used for fuels and chemicals supply at different times during petroleum shortage. For example, it has been reported the production of hydrocarbons from Tung oil in China during the Second World War.[11] Since then, numerous studies about the thermal[12-18] and catalytic[19-29] pyrolysis of triglycerides and

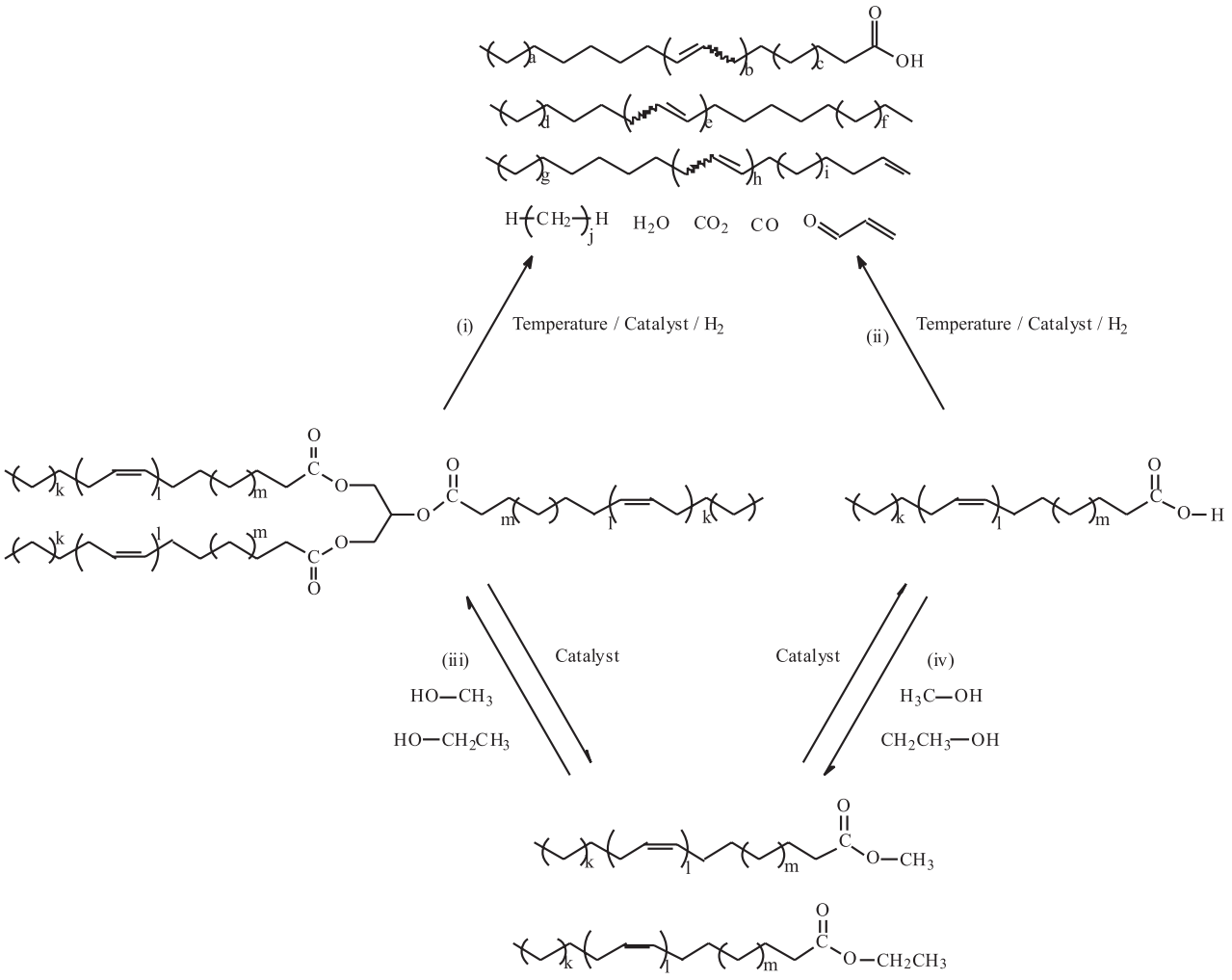

Figure 1. Processing fatty acids and their derivatives into alternative fuels: (i) pyrolysis of triglycerides; (ii) pyrolysis of fatty acids; (iii) alcoholysis of triglycerides; and (iv) alcoholysis of fatty acids. Adapted from reference 10.

fatty acids have been developed. It was proposed that the decomposition of the glyceridic fragment of the triglyceride achieves carboxylic acids, acrolein and ketenes.[6,11,20,26] At the employed reaction conditions, these oxygenated compounds are further decomposed affording esters, carboxylic acid and hydrocarbons. Thus, the carboxylic acids are decarboxylated or decarbonylated, producing, respectively, carbon dioxide and paraffins or carbon monoxide, olefins and water.[20] It is also recognized that several side and consecutives reactions take place, such us cracking of C-C bonds, cyclization, dehydrogenation, aromatization and radical oligo-polymerization.[6] When the pyrolysis is carried out thermally, the characterization of the products indicated that the reaction affords a complex mixture containing high amounts of inconvenient oxygenated compounds, such as aldehydes and carboxylic acids. The presence of these oxygenated compounds are partially or completely reduced when the reaction is carried out in the presence of a catalyst.[8] For instance, it was observed that the presence of different types of zeolites dramatically changes the reaction products,[21,24-26,28] affording essentially non-oxygenated compounds, mainly aromatic and short chain hydrocarbons in the range of gasoline.[19,22] On the other hand, it was also reported that the products of soybean and babassu oils pyrolysis catalyzed by γ-alumina doped with nickel and molybdenium were completely deoxygenated when the reaction was carried out in the presence of hydrogen pressure.[20]

The production of mono-alcohol fatty acid esters by transesterification of vegetable oils with short chain mono-alcohols, generating glycerin as a by product, is well studied and established using homogeneous Brønsted acids or alkali catalysts, like alkali metal hydroxides or alkoxides and sulfuric acid.[6,8] However, these catalytic systems have some technological problems, being the acid system associated with corrosion and the basic one with emulsification. In fact, the soaps formed when using basic catalysis are known to emulsify the biofuels with glycerin, especially if ethanol

is used. Furthermore, these catalytic systems are less active or completely inactive for ethanol and high molecular weight alcohols.[30] In order to minimize these problems, attempts to use homogeneous and heterogeneous Lewis acid metal compounds as catalyst systems in the alcoholysis of triglycerides, as well as enzymatic catalysis, have been made.[8,31] The heterogeneous systems are active for high molecular weight alcohols, achieving conversions higher than 95% in systems where neither alkali nor acid catalysts work and produce neither corrosion nor emulsion, making easier to separate the products obtained and recover and reuse the catalysts.[32,33]

Mono-alcohol fatty acids esters can also be obtained by esterification of fatty acids. Indeed, this technological approach has been proposed as a viable solution for raw materials with high free fatty acids contents.[34] Some reports are available in the literature describing homogeneous and heterogeneous catalytic systems for the esterification of fatty acids.[35-41] The homogeneous ones, usually strong minerals acids, are associated to problems of equipments corrosion and difficulties in the products separation. The heterogeneous ones are associated to low activity due to phase transfer. Therefore, the technological challenge for fatty acids esterification process is the development of high active heterogeneous acid catalysts, easy to recover from the products and with no corrosion issues.

Niobium oxide and its acid derivatives obtained by treatment with water and inorganic acids such as phosphoric and sulfuric acids are known to have a great acidity and have been described as suitable acid catalysts for several reactions. Indeed, they have been used in hydration, dehydration, esterification, hydrolysis, condensation, etc., and some reviews on these uses are already available.[42,43] However, as far as we know, there are few reports in the literature regarding to the use of niobium oxide and its derivatives as catalysts for biofuels productions. The hydrated niobium oxide (niobium acid) is described as active for the esterification of a mixture containing 80% of free fatty acid as obtained after a physical refining of palm oil.[44] It has also been observed that the use of this catalyst and some derivatives of it in the pyrolysis of soybean oil lead to an increase in the catalyst acidity decreases.[45]

Our goal in this work was to develop new heterogeneous catalytic systems for the esterification, transesterification and pyrolysis of vegetable oils and fatty acids using niobium oxide and its acidic derivatives. In this sense, we have prepared some derivatives by treating hydrated niobium oxide ($Nb_2O_5{\cdot}H_2O$) with sulfuric acid (Nb_2O_5/H_2SO_4), phosphoric acid (Nb_2O_5/H_3PO_4) and nitric acid (Nb_2O_5/HNO_3). It is worth to mention that as far as it is our knowledge this is the first report of the Nb_2O_5/HNO_3 compound. The obtained materials have been characterized by thermal analysis (DTA-TGA), spectroscopy (X-ray, FT-IR and FT-Raman), surface area (BET) and the acidity (Ho) determined by *n*-butylamine titration using the Hammet indicator method.

Experimental

Catalysts preparation

Nb_2O_5 and $Nb_2O_5{\cdot}H_2O$ were obtained from Companhia Brasileira de Metalurgia e Mineração-CBMM and used without further purification. All other chemicals were purchased from commercial sources and use as received.

Nb_2O_5/H_2SO_4 derivative was prepared using a modified method described in the literature.[42] $Nb_2O_5{\cdot}H_2O$ (3 g) was added to a 12 mol L^{-1} sulfuric acid solution (6 mL) in an ampoule. After sealing it, the mixture was kept standing for 48 hours in an oven for 48 h at 110 °C. The solid was washed with distilled water until no sulfate ion was detected (tested using a 0.05 mol L^{-1} barium chloride solution) and then dried in an oven for 24 h at 110 °C.

Nb_2O_5/H_3PO_4 derivative was prepared according to method described in the literature.[46] $Nb_2O_5{\cdot}H_2O$ (3 g) was added to a 1 mol L^{-1} phosphoric acid solution (10 mL) and then kept standing for 48 h under ambient temperature. Then, the mixture was dried in an oven for 48 h under 110 °C.

Nb_2O_5/HNO_3 was prepared using a similar procedure as described for $Nb_2O_5{\cdot}H_3PO_4$.[46] $Nb_2O_5{\cdot}H_2O$ (3g) was added to a 1 mol L^{-1} nitric acid solution (10 mL) and then kept standing for 48 hours under ambient temperature followed by drying in an oven for 48 h at 110 °C.

All the obtained solids were finally atomized and sieved (diameter ≤ 400 μm).

Catalysts characterization

The surface acidity of catalysts was determined by the Hammet indicator method,[47] using bromothymol blue, methyl yellow and violet crystal under nitrogen atmosphere. Three indicators solutions were prepared by dissolving each one (0.2 mg) in freshly distilled carbon tetrachloride (100 mL). Under nitrogen atmosphere, the solids (0.1 g) were mixed with the different indicator solutions (5 mL). The nine different mixtures were then titrated using a 0.05 mol L^{-1} solution of *n*-butyl amine dissolved in carbon tetrachloride.

The solids were characterized by X-rays powder diffraction (XRD). The XRD patterns were collected using

a Rigaku D/Max-2A/C with Cu Kα radiation at 40 KV and 20 mA. A 2θ range from 2° to 70 ° was scanned at 2° min^{-1}. The different niobium oxides were characterized by thermal analysis using SDT 2960 TA-Instruments (simultaneous DSC-DTA-TGA) equipment, under N_2 flux, using a heating rate of 10 °C min^{-1}, at temperatures varying from 50 to 800 °C. The surface areas of the different niobium oxides were obtained by BET method using a Micrometrics analyzer model ASAP-2010. The isotherms were obtained through adsorption of N_2 at 77.30 K.

FT-Raman spectra of powder samples were obtained on an Equinox 55 interferometer from Bruker equipped with a Raman accessory and a Ge detector cooled with liquid N_2. The FT-Raman spectra were excited at 1064 nm from a NdYag laser (Bruker) operated at 150 mW. Each spectrum is the average of 128 scans at a nominal spectral resolution of 8 cm^{-1}. The same instrument was used to record FT-IR spectra from samples in KBr pellets using a DTGS detector. Each FT-IR spectrum is the average of 32 scans at a nominal spectral resolution of 4 cm^{-1}.

Transesterification reactions

The vegetable oil (10 g) was transesterified in the presence of different alkyl-chain alcohols (2.0 g) and one of the different niobium solids (0.1 g). The reaction mixtures were kept in a 50 mL batch reactor under reflux and magnetic stirring for the desired time. The product obtained was washed three times with distilled water and the recovered esters were analyzed by gas chromatography on a Shimadzu GC-17A chromatograph equipped with FID detector, a polydimethylsiloxane column (CBPI PONA-M50-042, 50 m, 0.25 mm i.d. and film thickness of 0.2 μm), at temperatures varying from 80 to 180 °C, with a heating rate of 10 °C min^{-1}, using ethyl acetate (0.1 g) as internal standard.

Esterification reactions

A fatty acids mixture was obtained through saponification of soybean oil using sodium hydroxide followed by acidification with hydrochloric acid. The mixture was washed with water and dried with magnesium sulfate. The composition of this fatty acid mixture as determined by HPLC using a method described elsewhere[48] was in the range expected for soybean oil (linoleic acid, 52%; oleic acid, 24%; palmitic acid, 14%; stearic acid, 4%; other acids, 6%).

The esterification reactions were carried out in a home-made stainless steel autoclave. The catalyst and the fatty acid mixture were inserted in the reactor through a valve. The methanol was in a stainless steel reservoir connected to the reactor by a valve. Under constant magnetic stirring, the reactor was heated until the desired temperature was achieved. The temperature was monitored with a thermocouple inserted in a stainless steel cold finger in contact with the reaction bulk. At the desired temperature, methanol was introduced into the reactor and the reaction started. At the determined time, the reaction was stopped by turning of the stirring and heating. The product was then dried in a rotaevaporator to ensure complete removal of residual water and methanol. Reactions yields were calculated based on the diminishing of acid index for products in relation to acid index for the initial fatty acids mixture. All acid indexes were determined according to AOCS Cd3d63 specification.[49]

Pyrolysis reactions

The pyrolysis reaction was carried out in a three necked round bottom flask connected to a glass condenser tube and a graduated collector, as indicated in Figure 2. Two thermocouples were used to control the temperature of the reaction and of the vapors leaving the system. Both the vegetable oil (100 g) and the catalyst (1 g; the catalyst $Nb_2O_5 \cdot H_2O$ was also tested in the quantity of 0.5 g) were introduced in the flask and then heated by an electric resistance to maintain the reaction temperature between 350 °C and 400 °C. When the temperature in the flask reached 350 °C, the vegetable oil started to crack and the volatile products vaporized. The vapors left the flask with temperatures between 200 °C and 250 °C and were then condensed and collected. The whole reaction results in a non condensed gas, a very viscous residue and in two liquid phases: an aqueous and an organic one. The reaction was stopped when approximately 75% of liquid

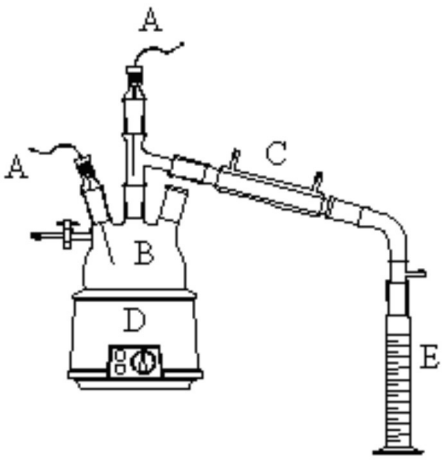

Figure 2. Scheme of the apparatus used in the pyrolysis experiments: (A) thermocouples, (B) three-neck round flask, (C) condenser, (D) oven, (E) graduated collector.

was recovered. After decantation of the two liquid phases, the organic one was submitted to a fractioned distillation in order to separate four distinct fractions by their distillation temperature (DT) range as follows: F1 (DT < 80 °C), F2 (80 °C < DT < 140 °C), F3 (140 °C < DT < 200 °C) and F4 (DT > 200 °C). This procedure was carried out in a common system for fraction distillation.

All fractions were analyzed by gas chromatography, FT-IR and the acid number. The gas chromatography analysis were carried out in a Shimadzu GCMS-QP5050 equipped with a mass spectrometer containing a polydimethylsiloxane column 50 m, 0.25 mm id and 0.2 μm thin layer (CBPI PONA-M50-042), operating between 50 ºC and 250 ºC with a heating rate of 10 ºC min^{-1}. The FT-IR spectra from a thin layer of the biofuels in a NaCl window were obtained on a Bruker Equinox 55. The FTIR spectrum corresponds to the sum of 64 scans with a spectral resolution of 4 cm^{-1}. The acid number was determined by ASTM D465-9.

Results and Discussion

Catalysts characterization

Surface areas were obtained for the different solids by B.E.T and Langmuir methods. The results are displayed in Table 1. The results clearly show that the surface area decreases dramatically with the acid treatment of the $Nb_2O_5{\cdot}H_2O$, which was already reported in the literature.[46] It is worth mentioning that the surface area increases in the following order $Nb_2O_5 < Nb_2O_5/H_2SO_4 < Nb_2O_5/H_3PO_4 < Nb_2O_5/HNO_3 < Nb_2O_5{\cdot}H_2O$.

Table 1. BET and Langmuir surface areas for the different niobium oxides

Solid	BET / (m^2 g^{-1})	Langmuir / (m^2 g^{-1})
Nb_2O_5	1.1	1.8
Nb_2O_5/H_2SO_4	9.3	12.9
Nb_2O_5/H_3PO_4	50.1	71.0
Nb_2O_5/HNO_3	101.6	144.3
$Nb_2O_5{\cdot}H_2O$	162.2	225.0

The surface acidity of the niobium solids was measured by the *n*-butylamine titration method using the Hammett indicators with $-3.3 < Ho < +0.8$. It was observed that the acidity decreases in the order $Nb_2O_5/H_3PO_4 > Nb_2O_5/H_2SO_4 > Nb_2O_5{\cdot}H_2O > Nb_2O_5/HNO_3$. Note that for the Nb_2O_5/H_3PO_4 $Ho < -3.3$ and for the $Nb_2O_5{\cdot}HNO_3$ the $Ho > +0.8$. Using other Ho ranges, similar surface acidities for the compounds, $Nb_2O_5/H_3PO_4 > Nb_2O_5/H_2SO_4 > Nb_2O_5{\cdot}H_2O$, were reported in the literature.[42]

XRD pattern of the Nb_2O_5/H_3PO_4 is presented in Figure 3A and shows the formation of a crystalline phase. The other niobium compounds $Nb_2O_5{\cdot}H_2O$, Nb_2O_5/H_2SO_4 and Nb_2O_5/HNO_3 present XRD patterns characteristic of amorphous material as can be seen for the $Nb_2O_5{\cdot}H_2O$ (see Figure 3B).

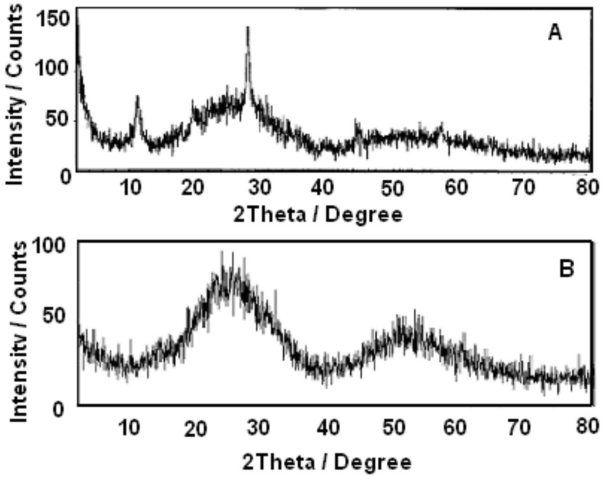

Figure 3. X-rays diffratogram patterns for (A) Nb_2O_5/H_3PO_4 and (B) $Nb_2O_5{\cdot}H_2O$.

TGA/DTA/DSC profiles obtained for the different solids are shown in Figure 4. All DTA curves present a weak and broad feature near 200 °C, accomplished by a continuous loss of mass in the TGA curve, which can be attributed to the dehydration of the samples. For the $Nb_2O_5{\cdot}H_2O$ an exothermic sharp peak was observed at 566.14 °C, Figure 4a, which can be associated to the formation of a crystalline phase. It seems that this peak is sensitive to the acidic treatments. For instance, in the DSC curve of Nb_2O_5/H_2SO_4, Figure 4b it appears close to 600 ºC as a broad exothermic feature and in the DSC curve of Nb_2O_5/HNO_3 sample, Figure 4d, this peak appears almost in the same position as in $Nb_2O_5{\cdot}H_2O$. However, this peak is not observed in the DSC curve of Nb_2O_5/H_3PO_4, Figure 4c. This effect was already described in the literature[42] and is associated with a suppression of the crystallization due to the phosphoric acid treatment. However, the crystalline properties of this solid were not investigated in reference 42. As shown in Figure 3a, the Nb_2O_5/H_3PO_4 sample is already crystalline from the beginning which explains why no phase transition is observed in Figure 4c. On the other hand the Nb_2O_5/H_2SO_4 sample shows a loss of mass just above of 600 °C, which can be due to sulfuric acid decomposition.

FT-Raman spectra of the investigated catalysts are displayed in Figure 5. The main observed Raman features and relative intensities of the hydrated and acid treated

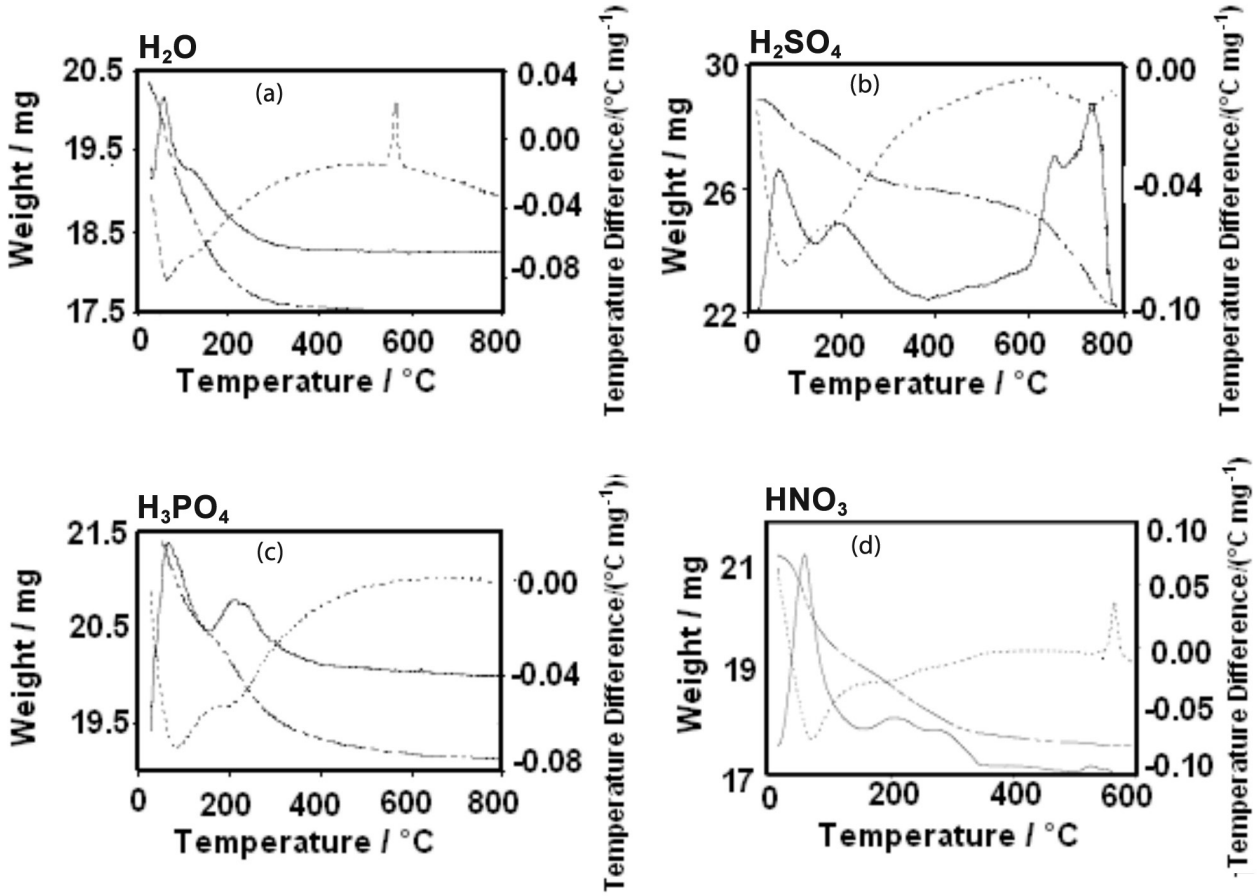

Figure 4. TGA/DTA/DSC profiles obtained for the solids: (a) $Nb_2O_5 \cdot H_2O$, (b) Nb_2O_5/H_2SO_4, (c) Nb_2O_5/H_3PO_4 and (d) Nb_2O_5/HNO_3. (— - - —) TG; (———) DTA; (- - - - - -) DSC.

catalysts are presented in Table 2. The Raman spectrum of the Nb_2O_5 sample presents a large number of Raman bands, with well defined peaks, that can be explained by the high crystallinity of the substrate as evidenced by the X-ray analysis. The observed Raman bands are in quite good agreement with the data reported in the literature for this species.[50,51] On the other hand, the hydrated niobium oxide ($Nb_2O_5 \cdot H_2O$) is amorphous, and its Raman spectrum presents not well defined bands, that is, the observed Raman features are very broad. The Raman band at *ca.* 640 cm^{-1} (the Nb-O stretching) matches that of the slightly distorted NbO_6 octahedral present in amorphous $Nb_2O_5 \cdot nH_2O$.[50]

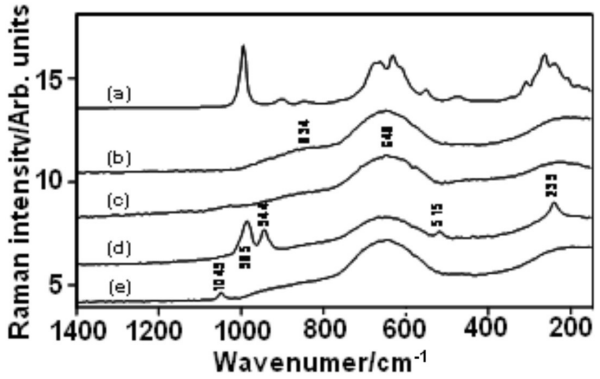

Figure 5. FT-Raman spectra of: (a) Nb_2O_5; (b) $Nb_2O_5 \cdot H_2O$; (c) Nb_2O_5/H_2SO_4; (d) Nb_2O_5/H_3PO_4; (e) Nb_2O_5/HNO_3.

According to Franklin *et al.*,[52] the medium intensity broad feature at *ca.* 834 cm^{-1} extending up to 900 cm^{-1} in the Raman spectrum of the hydrated niobate species is due to a highly distorted NbO_6 octahedron of an aqueous $H_xNb_6O_{19(8-x)}$- surface species. These authors came to this conclusion by comparing the Raman spectra of known aqueous niobate reference compounds[53] with the spectrum of the hydrated niobate species. Note that these broad Raman features are observed in all other Nb_2O_5 catalysts treated with different acids. Besides these two broad features new Raman peaks emerge upon acidic treatments that are also displayed in Table 2.

FT-IR spectra of the investigated samples are presented in Figure 6 and the wavenumbers corresponding to each one of the absorptions is displayed in Table 3.

The absorptions at 640 and *ca.* 900 cm^{-1} can be assigned to the same vibrational modes corresponding to the similar Raman features observed in the Raman spectra of these

Table 2. Raman signals (in cm^{-1}) observed in the Raman spectra of the investigated catalysts

$Nb_2O_5 \cdot nH_2O$	Nb_2O_5/H_2SO_4	Nb_2O_5/H_3PO_4	Nb_2O_5/HNO_3
		239 (s)*	
	427 (vw)		
		515 (m)	
646 (vbr)	646 (vbr)	646 (vbr)	646 (vbr)
ca. 834 (mbr)	*ca.* 834 (mbr)	*ca.* 834 (mbr)	*ca.* 834 (mbr)
		944 (s)	
		985 (vs)	
	1024 (w)		
			1048 (w)

*relative intensities: w = weak; vw = very weak; m =medium; s = strong; vs = very strong; vbr = very broad; sh = shoulder.

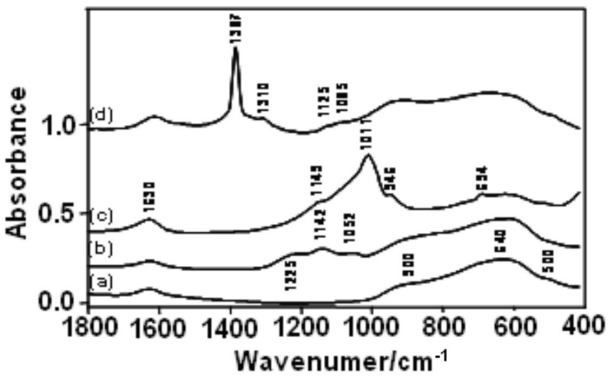

Figure 6. FT-IR absorption spectra (KBr pellets) of: (a) $Nb_2O_5 \cdot H_2O$; (b) Nb_2O_5/H_2SO_4; (c) Nb_2O_5/H_3PO_4; (d) Nb_2O_5/HNO_3.

Table 3. IR absorptions observed in the FT-IR spectra of the investigated catalysts

$Nb_2O_5 \cdot nH_2O$	Nb_2O_5/H_2SO_4	Nb_2O_5/H_3PO_4	Nb_2O_5/HNO_3
ca. 500 (wsh)*	*ca.* 500 (wsh)	*ca.* 500 (wsh)	*ca.* 500 (wsh)
640 (vbr)	640 (vbr)	640 (vbr)	640 (vbr)
		694 (w)	
ca. 900 (br)	*ca.* 900 (br)	*ca.* 900 (br)	*ca.* 900 (br)
		946 (sh)	
		1011 (s)	
	1052 (m)		1085 (wsh)
	1142 (m)	1149 (sh)	1125 (wsh)
	1225 (m)		
			1310 (w)
			1387 (vs)
1630 (m)	1630 (m)	1630 (m)	

* Relative intensities as in Table 2.

samples. These features as well as the shoulder observed at *ca.* 500 cm^{-1} are characteristic of the $Nb_2O_5 \cdot H_2O$ catalyst.[54] The absorption observed at 1630 cm^{-1} corresponds to the HOH bending mode of the water present in the catalyst. Furthermore, new absorptions emerge upon acidic treatments which are also displayed in Table 3.

Tetrahedrally-coordinated PO, and SO, moieties are generally present in phosphorous and sulfurous compounds while octahedrally-coordinated P and S moieties are scarcely observed.[55] Table 4 shows the wavenumbers and vibrational assignment of Raman bands observed in the Raman spectra of some phosphate containing compounds. Based on these data the Raman features observed at 944 and 985 cm^{-1} in the Raman spectrum of the Nb_2O_5/H_3PO_4 catalyst (see Table 2) are tentatively assigned to the symmetric P=O-H and P=O stretching modes, respectively of a protonated tetrahedrally coordinated phosphate incorporated into the catalyst. The respective asymmetric stretching modes are observed in the FT-IR spectrum at 1011 and 1149 cm^{-1} (see Table 3). It is worth to mention that Amaroli *et al.*[54] have observed strong absorptions between 1040 and 1100 cm^{-1} in the IR spectra of niobate catalysts treated with phosphoric acid which were assigned to the O=P=O asymmetric stretching modes of phosphate or polyphosphate species.

Table 4. Raman shifts observed for phosphate compounds

	Symmetric P=O	Asymmetric P=O	Symmetric P=OH	Asymmetric P=OH
H_3PO_4 [(a)]	1170		891	1010
$H_2PO_4^-$ [(a)]	1078	1159	878	943
HPO_4^{2-} [(a)]	990	1084	858	
PO_4^{3-} [(a)]	938	1010		
$(Gd_2O_3)_{0.22}$				
$(P_2O_5)_{0.78}$ [(b)]	1194	1260	683 (POP) sym	
$NbOPO_4$ [(c)]	980	1016		

[(a)]ref. 56; [(b)]ref. 57; [(c)]ref. 58.

In order to get additional information from the FT-Raman spectrum of the Nb_2O_5/H_2SO_4 catalyst the Raman spectrum of the $Nb_2O_5 \cdot H_2O$ sample was subtracted from the one of Nb_2O_5/H_2SO_4. These spectra are displayed in Figure 7. In the difference spectrum two weak features are observed at *ca.* 427 and 564 cm^{-1} and a broad and more intense Raman signal appears at 1024 cm^{-1}. For comparison purposes Table 5 presents some Raman peaks observed in the Raman spectra of sulfate compounds. Note that one of the $CsHSO_4$ crystal forms present Raman signals that coincide with those that appear in the difference spectrum of Figure 7. Therefore, the Raman feature at 1024 cm^{-1} is

tentatively assigned to the symmetric stretching mode and the weak features at 427 and 564 cm^{-1} are assigned to the ν_2 and ν_4 modes, respectively, of HSO_4^- incorporated in the Nb_2O_5/H_2SO_4 catalyst.

Table 5. Raman and IR vibrational bands observed in some sulfate compounds

	$\nu_s(SO_4)$	S=OH stretching	$\nu_4(SO_4)$	$\nu_2(SO_4)$
$CsHSO_4$ (II)[a]	1021	855	588	428
$CsHSO_4$ (III)[a]	998	860	588	420
$KHSO_4$[b]	1009	873		
$S_2O_7^{2-}$ [(c)]	1035			

[a]ref. 59, II and III are two different crystalline phases; [b]ref. 59; [c]ref. 60

FT-IR spectrum of $CsHSO_4$ presents an absorption band observed near 1250 cm^{-1} that was assigned to the asymmetric S=OH stretching mode.[59] Besides this band two other features appears at 1175 and 1060 cm^{-1}, the later is assigned to the asymmetric S=O stretching.[59] Therefore the absorption features at 1225, 1142 and 1052 cm^{-1} observed in the IR spectrum of the niobium catalyst treated with sulfuric acid are assigned to the respective vibrational modes of HSO_4^- bounded to the catalyst surface.

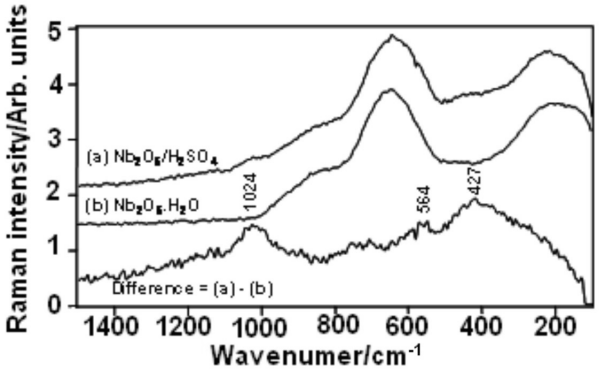

Figure 7. FT-Raman spectra of : (a) Nb_2O_5/H_2SO_4; (b) $Nb_2O_5 \cdot H_2O$ and the difference spectrum (a)-(b).

The symmetric NO stretching mode, ν_1, of NO_3^- is very strong in the Raman spectrum.[61] Therefore, the Raman feature at 1048 cm^{-1}, observed in the Raman spectrum of the Nb_2O_5/HNO_3 catalyst, is assigned to the ν_1 vibrational mode of NO_3^-. Another characteristic nitrate vibration is the ν_3 vibrational mode that is doubly degenerate at D_{3h} symmetry (appearing at ca 1380 cm^{-1}), being strong in the infrared and weak in the Raman spectrum. This mode splits into two absorptions in the infrared spectrum, one close to 1400 cm^{-1} and another at lower wavenumbers (1300 to 1350 cm^{-1}) when the symmetry is reduced.[62] In this sense, the absorption features at 1387 and 1310 cm^{-1} observed in the IR spectrum of Nb_2O_5/HNO_3 catalyst are assigned to the splitting of the ν_3 mode caused by a reduction in the symmetry (probably C_{2v}) of the nitrate ion upon incorporation into the catalyst. We believe that the HNO_3 species is not present on the catalyst surface rather the NO_3^- anion since the HNO_3 strong Raman signal[63] near 949 cm^{-1} was not observed which could then explain the lower acidity of the Nb_2O_5/HNO_3 catalyst in comparison to the others. We have no assignment for the weak features observed at 1085 and 1125 cm^{-1}. If we enlarge the infrared spectrum of the $Nb_2O_5 \cdot H_2O$ species, similar weak features are observed in this region.

Transesterification results

The different niobium oxides were tested as catalysts for the transesterification of soybean oil and the main results are summarized Table 6. The results show that all solids are active for the methanolysis reaction (see entries 1-20). Nonetheless, the most active catalyst using comparable conditions is the Nb_2O_5/H_3PO_4. This catalyst does not present the largest surface area among the investigated catalysts. Therefore, its higher activity can only be explained by its higher acidity when compared to the other solids. Indeed, this result is in good agreement with the acid mechanism proposed for this reaction.[64] The Nb_2O_5/H_3PO_4 was also tested as catalyst for the transesterification of soybean oil using other alcohols with longer alkyl chains (see entries 3 and 21-23 of Table 6). Not surprisingly, the catalytic activity decreases when the alkyl chain increases, which is associated in the literature with steric effects.[65]

Esterification results

The different niobium oxides were tested as catalysts for the esterification of fatty acid and the main results are summarized Table 7. Although fatty acids are weak Bronsted acids they are active catalysts in the esterification, being usually observed self-catalytic activity.[64] Thus, for the sake of comparison, the reaction was also carried out without any niobium catalyst.

The results of Table 7 show that only $Nb_2O_5 \cdot H_2O$ is inactive in comparison with the reaction without catalyst. Nonetheless, the catalytic activity of the different catalysts can be ordered as: $Nb_2O_5/H_3PO_4 = Nb_2O_5/H_2SO_4 > Nb_2O_5/HNO_3$, which is in good agreement with the surface acidity order. Thus, the mechanism of these reaction may be probably the usually accepted for esterification catalyzed by Lewis acid solids.[66] As proposed in Figure 8, niobium oxides reacts with methanol accepting electrons from the

Table 6. The transesterification of soybean oil using different alcohols catalyzed by the solids at different reaction times

Entry	Catalyst	Alcohol	Reaction time / min	ReactionYield / (%)
1	Nb_2O_5/H_3PO_4	MeOH	60	13.0
2	Nb_2O_5/H_3PO_4	MeOH	120	14.0
3	Nb_2O_5/H_3PO_4	MeOH	180	12.5
4	Nb_2O_5/H_3PO_4	MeOH	360	6.0
5	Nb_2O_5/H_2SO_4	MeOH	60	2.7
6	Nb_2O_5/H_2SO_4	MeOH	120	5.0
7	Nb_2O_5/H_2SO_4	MeOH	180	1.3
8	Nb_2O_5/H_2SO_4	MeOH	360	2.7
9	Nb_2O_5/HNO_3	MeOH	60	1.0
10	Nb_2O_5/HNO_3	MeOH	120	5.0
11	Nb_2O_5/HNO_3	MeOH	180	5.0
12	Nb_2O_5/HNO_3	MeOH	360	5.5
13	$Nb_2O_5{\cdot}H_2O$	MeOH	60	1.0
14	$Nb_2O_5{\cdot}H_2O$	MeOH	120	6.0
15	$Nb_2O_5{\cdot}H_2O$	MeOH	180	3.0
16	$Nb_2O_5{\cdot}H_2O$	MeOH	360	0.5
17	Nb_2O_5	MeOH	60	1.0
18	Nb_2O_5	MeOH	120	5.0
19	Nb_2O_5	MeOH	180	3.0
20	Nb_2O_5	MeOH	360	3.0
21	Nb_2O_5/H_3PO_4	EtOH	180	8.0
22	Nb_2O_5/H_3PO_4	2-prOH	180	2.0
23	Nb_2O_5/H_3PO_4	1-BuOH	180	1.0

MeOH = methanol, EtOH = ethanol, 2-prOH = 2-propanol, 1-BuOH = 1-butanol. Conditions: 10.0 g of soybean oil, 0.1 g of catalysts and 2.0 g of alcohol under reflux.

Table 7. The esterification of soybean fatty acids with MeOH catalyzed by the niobium solids*

Catalyst	Reaction Yield / (%)
without catalyst	32
$Nb_2O_5{\cdot}H_2O$	32
Nb_2O_5	36
Nb_2O_5/HNO_3	40
Nb_2O_5/H_3PO_4	57
Nb_2O_5/H_2SO_4	57

*Reaction conditions: 10 g of soybean fatty acids, 4 g of MeOH, 1 hour, 160 °C.

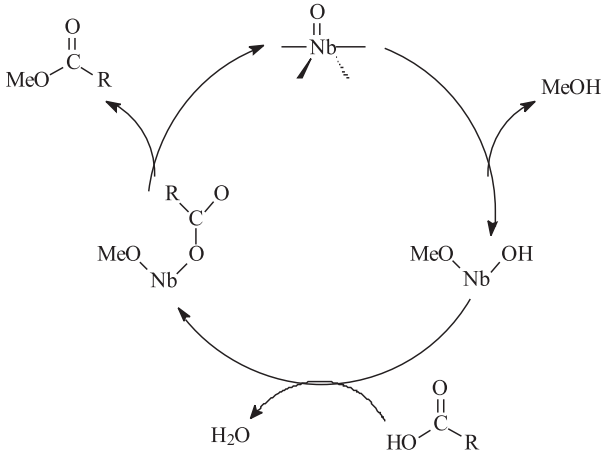

Figure 8. Proposed mechanism for esterification using niobium based catalysts.

alcohol, affording a hydroxyl and a methoxyl groups. Thus, the fatty acid reacts with the hydroxyl group leading to a carboxylate coordinated group. After a nucleofilic attack by the methoxy group to the carbonyl, the fatty acid ester is formed and the active oxide is recovered.

The inactivity of the $Nb_2O_5{\cdot}H_2O$ in the esterification, even having a higher acidity of the active $Nb_2O_5{\cdot}HNO_3$, can be explained by the strong interaction of the water in the catalytic center, hindering the coordination of the alcohol, as proposed in Figure 8. Indeed, the reaction of water with niobium oxide would form hydroxyl groups and, thus,

Table 8. Soybean oil pyrolysis' yields with different niobium oxide catalysts

Catalyst	Yield / (%)							
	OLP + water	OLP without water	Water	F1	F2	F3	F4	Gas
$Nb_2O_5 \cdot H_2O$ (0.5%)	46.2	42.7	3.5	1.5	1.3	1.6	38.2	5.7
$Nb_2O_5 \cdot H_2O$	74.5	72.0	2.5	3.1	5.6	12.7	50.6	1.5
Nb_2O_5	66.3	65.0	1.3	1.2	6.3	12.0	41.4	10.9
$Nb\text{-}H_3PO_4$	65.7	62.8	2.9	2.8	5.8	8.8	45.4	11.4
$Nb\text{-}H_2S0_4$	63.8	60.0	3.8	4.0	6.4	9.0	40.6	13.2
$Nb\text{-}HNO_3$	65.3	62.0	3.3	1.4	5.5	12.4	42.7	8.6

making difficult the formation of a methoxyl group. Note that if only hydroxyl groups are present in catalytic site, the final product is a fatty acid molecule instead of a fatty acid ester. It is also important to note that probably the water formed in the reaction process inactivates the catalyst, thus explaining the low catalytic activity of the solids.

Pyrolysis results

The reaction yields obtained for the different catalytic pyrolysis fractions of soybean oil with the different niobium oxide catalysts are presented in Table 8 and Table 9 show the acid number for respective fraction 4. The results of Table 8 show very similar yields of recovered organic liquid phase (OLP) and fraction 4 except for the $Nb_2O_5 \cdot H_2O$ catalyst that at the same conditions presented higher yields on both OLP and fraction 4. On the contrary, when used in less quantity (0.5 g), a lower yield was observed for both parameters. The distribution of the other fractions was quite similar for all the catalysts.

As far as the acid number is regarded, it can be seen that all the values presented in Table 9 are higher than the acidity index measured for product of soybean oil pyrolysis carried out using similar experimental conditions and in the absence of any catalyst.[18] This means that none of the catalysts tested in this work was active for the deoxygenation of pyrolysis products. It is difficult to correlate the catalyst surface area and acidity with the degree of decarbonylation/decarboxylation reaction of the carboxylic acids during the pyrolysis reaction. Idem and co-workers[24,26] have pointed out that there is a great controversy in the role of the catalyst surface area and acidity in the catalytic activity and products selectivity. Furthermore, there is a reasonable correlation between the integration of the IR absorption band corresponding the C=O stretching and the acid number measured for each catalyst tested, suggesting that free carboxylic acids are present in the products and that the amount of these compounds could be related to the area calculated for that specific peak.

Table 9. Acid number (AN, mg KOH g^{-1}) and integrated intensity of C=O stretching signal at 1710 cm^{-1} of diesel fractions obtained with different catalysts

Catalyst	AN	Max/min normalized C=O/C-H
$Nb\text{-}H_2O$ (0.5%)	237	1.00
$Nb\text{-}H_2O$	172	0.51
$Nb\text{-}HNO_3$	154	0.47
$Nb\text{-}H_3PO_4$	126	0.09
$Nb\text{-}H_2SO_4$	120	0.03
Nb_2O_5	121	0.00
None	116	-

FT-IR spectra of the products present in the diesel fraction, F4 (> 200 °C) for each catalyst tested are displayed in Figure 9. It can be observed, in the 2840-3000 cm^{-1} region, absorption bands associated with the CH stretching modes of aliphatic hydrocarbons. Deconvolution of the base lines show a broad background in the 2500-3400 cm^{-1} spectral range that is characteristic of OH stretching mode of hydrogen bonded carboxylic acids. The IR absorption at 1710 cm^{-1} is the C=O stretching mode. Since the spectra in Figure 10 were normalized in relation to the intensity of the CH_3 bending signal at 1459 cm^{-1}, it is also possible to compare the intensity of the C=O stretching of the products obtained with the tested catalysts. The following order of increasing intensity was observed: $Nb_2O_5 < Nb_2O_5/H_2SO_4 < Nb_2O_5/H_3PO_4 < Nb_2O_5/HNO_3 < Nb_2O_5 \cdot H_2O < Nb_2O_5 \cdot H_2O$ (0.5%), which matches almost perfectly with acid number data, except for Nb_2O_5 and Nb_2O_5/H_2SO_4 catalysts.

GC-FID and GC-MS analyses of the diesel fractions showed that the catalytic pyrolysis results in a mixture of hydrocarbons with long, linear and saturated or unsaturated chains. It was also observed the presence of oxygenated products such as linear carboxylic acids. In the fractions 1 and 2, the presence of saturated and unsaturated hydrocarbons with carbon chains smaller than C12 was

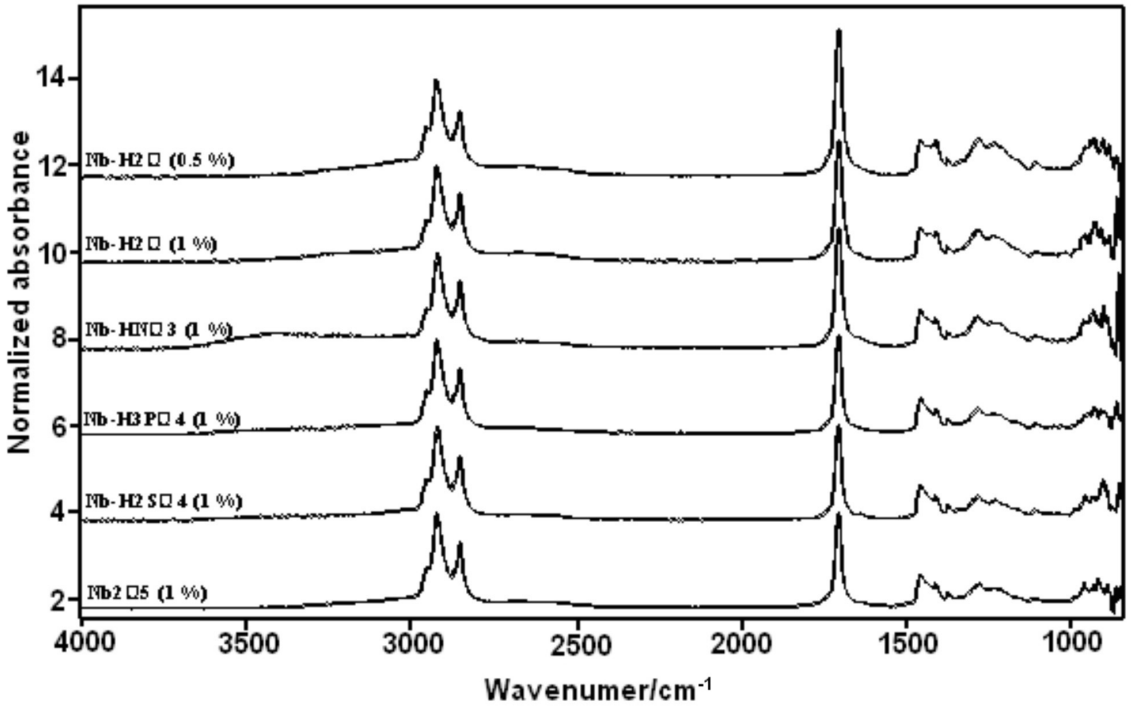

Figure 9. FT-IR spectra of diesel fractions obtained with the soybean oil pyrolysis assisted by niobium oxides catalysts.

observed. The presence of 2-propenal (acrolein) and 2-propanone was also detected in these fractions.

The presence of long chain carboxylic acids among the products of triglycerides pyrolysis has been reported by Nawar.[19] The formation of that kind of product is the result of the thermal cracking mechanism for triglycerides.[20] The presence of carboxylic acids in the reaction product makes it very acid and represents a disadvantage in the use of these catalysts to obtain diesel-like fuels. Even though the carboxylic acids are degradated during the process,[20] we can still verify a higher acid number for the pyrolysis products when using niobium oxides catalysts than when no catalyst is used. Similar behavior has already been described for niobium based catalyst[45] and other basic, MgO and CaO, catalysts.[26] This fact may be related to a sort of stabilization of the carboxylic function of these molecules by its interaction with the catalyst. Indeed, the basic sites of the catalyst structure would interact strongly with the acidic hydrogen of the carboxylic acids resulting in a very stable intermediate where the proton is midway between complete dissociation and attached to the carboxylate ion. This structure is stabilized by the resonance of the COO^- group.

Conclusions

In summary, it has been shown that the treatment of $Nb_2O_5 \cdot H_2O$ with different mineral acids affords niobium compounds with different surface area and acidity, being the most acid the one obtained with H_3PO_4, the only that presented crystalline characteristics. When tested for the soybean oil transesterification reaction, all solids presented catalytic activity. The higher catalytic activity was achieved in the methanolysis of soybean in the presence of Nb_2O_5/H_3PO_4. This compound was also tested using other alcohols, diminishing the catalytic activity with the increase in the alkyl chain, probably due to a steric hindrance effect. In the esterification process only $Nb_2O_5 \cdot H_2O$ revealed no activity while the Nb_2O_5/H_2SO_4 and Nb_2O_5/H_3PO_4 showed promising results.

The products of the catalytic pyrolysis of soybean oil consisted mainly of a mixture of linear hydrocarbons and oxygenated compounds, such as carboxylic acids. The presence of niobium oxide catalysts during the pyrolysis may account for the stabilization of the carboxylic acids structures increasing the acidity of the products obtained. The higher deoxygenating activity was achieved when the solid Nb_2O_5/H_2SO_4 was used in the reaction. Very small differences were observed in the distribution of the distillated fractions, especially for diesel-like fraction, suggesting that all tested catalysts act similarly in the pyrolysis of soybean oil.

Acknowledgments

The financial supports from CNPq, CTPETRO, Fundação Banco do Brasil, Embrapa and CAPES are

gratefully acknowledged. The authors also thank CBMM for the donation of niobium oxide and hydrated niobium oxide. PAZS, JCR, VMM, RFB and RLQ also thank CNPq for research fellowships.

References

1. Kirschbaum, M. U. F.; *Biomass Bioenergy* **2003**, *24*, 297.
2. Demirbas, A.; *Energy Convers. Manage*. **2006**, *47*, 2271.
3. Chisti, Y; *Biotechnol. Adv.* **2007**, *25*, 294.
4. Demirbas, M. F.; Balat, M.; *Energy Convers. Manage.* **2006**, *47*, 2371.
5. Abreu, F. R.; Lima, D. G.; Hamú, H. E.; Einloft, S.; Rubien, J. C.; Suarez, P. A. Z.; *J. Am. Oil Chem. Soc.* **2003**, *80*, 601.
6. Pinto, A. C.; Guarieiro, L. L. N.; Rezende, M. J. C.; Ribeiro, N. M.; Torres, E. A.; Lopes, W. A.; Pereira, P. A.; Andrade, J. B. de; *J. Braz. Chem. Soc.* **2005**, *16*, 1313.
7. Ma, F.; Hanna, M. A.; *Bioresour. Technol.* **1999**, *70*, 1.
8. Suarez, P. A. Z.; Meneghetti, S. M. P.; Meneghetti, M. R.; Wolf, C. R.; *Quim. Nova* **2007**, *30*, 667.
9. Pousa, G. P. A. G.; Santos, A. L. F.; Suarez, P. A. Z.; *Energy Policy* **2007**, *35*, 5393.
10. Suarez, P. A. Z.; Meneghetti, S. M. P.; *Quim. Nova* **2007**, *30*, 2068.
11. Chang, C.-C.; Wan, S.-W.; *Ind. Eng. Chem.* **1947**, *39*, 1543.
12. Alencar, J. W.; Alves, P. B.; Craveiro, A. A.; *J. Agric. Food Chem*. **1983**, *31*, 1268.
13. Fortes, I. C. P.; Baugh, P. J.; *J. Anal. Appl. Pyrolysis* **1994**, *29*, 153.
14. Santos, F. R.; Ferreira, J. C. N.; Costa, S. R. R. da; *Quim. Nova* **1998**, *21*, 560.
15. Schwab, A. W.; Dykstra, G. J.; Selke, E.; Sorenson, S. C.; Pryde, E. H.; *J. Am. Oil Chem. Soc*. **1988**, *65*, 1781.
16. Fortes, I. C. P.; Baugh, P. J.; *J. Braz. Chem. Soc.* **1999**, *10*, 469.
17. Schwab, A. W.; Dykstra, G. J.; Selke, E. S.; Sorenson, C.; Pryde, E. H.; *J. Am. Oil Chem. Soc*. **1988**, *65*, 1781.
18. Lima, D. G.; Soares, V. C. D.; Ribeiro, E. B.; Carvalho, D. A.; Cardoso, E. C. V.; Rassi, F. C.; Mundim, K. C.; Rubim, J. C.; Suarez, P. A. Z.; *J. Anal. Appl. Pyrolysis* **2004**, *71*, 987.
19. Nawar, W. W.; *J. Agric. Food Chem*. **1969**, *17*, 18.
20. Gusmão, J.; Brodzki, D.; Djéga-Mariadassou, G.; Frety, R.; *Catal. Today* **1989**, *5*, 533.
21. Sharma, R. K.; Bakhshi, N. N.; *Can. J. Chem. Eng.* **1991**, *69*, 1071.
22. Konar, S. K.; Boocock, D. G. B.; Mão, V.; Liu, J.; *Fuel* **1994**, *73*, 642.
23. Katikaneni, S. P. R.; Bakhshi, N. N.; Adjaye, J. D.; *Energy Fuels* **1995**, *9*, 599.
24. Idem, R. O.; Katikaneni, S. P. R.; Bakhshi, N. N.; *Energy Fuels* **1996**, *10*, 1150.
25. Prasad, Y. S.; Bakhshi, N. N.; Mathews, J. F.; Eager, R. L.; *Can. J. Chem. Eng.* **1986**, *67*, 278.
26. Idem, R. O.; Katikaneni, S. P. R.; Bakhshi, N. N.; *Fuel Process. Technol.* **1997**, *51*, 101.
27. Santos, F. R.; Ferreira, J. C. N.; Costa, S. R. R. da; *Quim. Nova* **1998**, *21*, 560.
28. Dandik, L.; Aksoy, H. A.; Erdem-Senatalar, A.; *Energy Fuels* **1998***, 12,* 1148.
29. Gomes, J. R.; *BR 0500591*, **2005**.
30. Demirbas, A.; *Energy Convers. Manage.* **2002**, *43*, 2349.
31. Fukuda, H.; Kondo, A.; Noda H.; *J. Biosci. Bioeng*. **2001**, *92*, 406.
32. Macedo, C. C. S.; Abreu, F. R.; Tavares, A. P.; Alves, M. B.; Zara, L. F.; Rubim J. C.; Suarez, P. A. Z.; *J. Braz. Chem. Soc.* **2006**, *17*, 1291.
33. Abreu, F. R.; Alves, M. B.; Macêdo, C. C. S.; Zara, L. F.; Suarez, P. A. Z.; *J. Mol. Catal. A: Chem.* **2005**, *227*, 263.
34. Keim, G. I.; *US patent 2,383-601* **1945.** (*CA* 1946, 40, 4617).
35. Marchetti, J. M.; Miguel, V. U.; Errazu, A. F.; *Fuel* **2007**, 906.
36. Kusdiana, D.; Saka, S.; *J. Chem. Eng. Jpn.* **2001**, *34*, 383.
37. Jackson, M. A.; Mbaraka, I. K.; Shanks, B. H.; *Appl. Catal., A* **2006**, *4*, 310.
38. Kiss, A. A.; Omota, F.; Dimian, A. C.; Rothenberg, G.; *Top. Catal.* **2006**, *40*, 141.
39. Minami, E.; Saka, S.; *Fuel* **2006**, *85*, 2479.
40. Mbaraka, I. K.; Shanks, B. H.; *J. Catal*. **2005**, *229*, 365.
41. Di Serio, T. M.; Guida, M.; Nastasi, M.; Santacesaria, E.; *Ind. Eng. Chem. Res*. **2005**, *44*, 7978
42. Guo, C.; Qian, Z.; *Catal. Today* **1993**, *16*, 379.
43. Nowak, I.; Ziolek, M.; *Chem. Rev.* **1999**, *99*, 3603.
44. Aranda, D. A. G.; Antunes, O. A. C.; *WO 2004096962*, **2004**.
45. Gonzalez, W. A.; Nunes, P. P.; Ferreira, M. S.; Martins, E. P.; Reguera, F. M.; Pastura, N. M. R.; *Encontro de Energia no Meio Rural,* Campinas, Brazil, 2000. Proceedings online, available from http://www.proceedings.scielo.br/scielo.php?script=sci_arttext&pid=MSC0000000022000000200047&lng=en&nrm=abn, accessed in December 2008.
46. Okazaki, S.; Kurosaki, A.; *Catal. Today* **1990**, *8*, 113
47. Noda, L. K.; *Quim. Nova* **1996**, *19*, 135.
48. Neto, B. A. D.; Alves, M. B; Lápis, A. A. M.; Nachtigall, F. M.; Eberlin, M. N.; Dupont, J.; Suarez, P. A. Z.; *J. Catal*. **2007**, *249*, 152.
49. American Oil Chemists' Society; *Official Methods and Recommended Practices of the American Oil Chemists' Society,* Champaign, 1993.
50. Ikeya, T.; Senna, M.; *J. Non-Cryst. Solids* **1988**, *105*, 243.
51. Kawano, Y.; Denofre, S.; Gushikem, Y.; *Vib. Spectrosc*. **1994**, *7*, 293.
52. Hardcastle, F. D.; Wachs, I. E.; *Solid State Ionics* **1991**, *45*, 201.

53. Goiffon, A.; Spinner, B.; *Rev. Chim. Min.* **1974**, *11*, 262.
54. Armaroli, T.; Busca, G.; Carlini, C.; Giuttari, M.; Galletti, A. M. R.; Sbrana, G.; *J. Mol. Catal. A: Chem.* **2000**, *151*, 233.
55. Kayo, A.; Yamaguchi, T.; Tanabe, K.; *J. Catal*. **1983**, *83*, 99.
56. Deng, H.; Wang, J.; Callender, R.; Ray, W. J.; *J. Phys. Chem.* B **1998**, *102,* 3617.
57. Koudelka, L.; Mosner, P.; *J. Non-Cryst. Solids* **2001**, *293*, 635.
58. Hardcastle, F. D.; Wachs, I. E.; *Solid State Ionics* **1991**, *45*, 201.
59. Sawatari, Y.; Sueoka, T. A.; Shingaya, Y.; ITO, M.; *Spectrochim. Acta, Part A* **1994**, *50*, 1555.
60. Fehrmann, R.; Hansen, N. H.; Bjerrum, N. J.; *Inorg. Chem*. **1983**, *22*, 4009.
61 Janz., G. J.; Kozlovski, T. R.; Wait, S. C.; *J. Chem. Phys*. **1963**, *39*, 1809.
62. Ferraro, J. R; *J. Mol. Spectrosc.* **1960**, *4*, 99.
63. Kamboures, M. A.; van der Veer, W.; Gerber, R. B.; Phillips, L. F.; *Chem. Phys*. **2008**, *10*, 4748.
64. Brito, Y. C.; Mello, V. M.; Macedo, C. C. S.; Meneghetti, M. R.; Suarez, P. A. Z.; Meneghetti, S. M. P.; *Appl. Catal., A* **2008**, *351*, 24.
65. Parshall, G. W.; Ittel, S. D.; *Homogeneous Catalysis-The Applications and Chemistry of Catalysis by Soluble Transition Metal Complexes*, John Wiley: New York, 1992.

Received: October 6, 2008
Web Release Date: April 24, 2009